JOURNAL OF MATERIALS SCIENCE 26 (1991) 6161–6170

Fatigue characteristics of pulsed MIG-welded Al–Zn–Mg alloy

P. K. GHOSH, S. R. GUPTA, P. C. GUPTA, R. RATHI
Welding Research Laboratory, Department of Mechanical and Industrial Engineering, University of Roorkee, Roorkee 247667, India

Pulse-current MIG welding of Al–Zn–Mg alloy was carried out using an extruded section of base material and Al–Mg (5183) filler wire. During welding the pulse parameters such as the mean current and pulse frequency were varied and their effect on the geometry and porosity content of weld deposit as well as the fatigue life of the weldment was studied. The pulse parameters were found to affect significantly the geometry and porosity content of weld deposit and consequently the fatigue life of the weldment. For a comparative study, weldments were also prepared by using conventional continuous current MIG-welding process, where welding currents equivalent to the mean currents of pulsed process were used. The fatigue life of the weldment was correlated with the geometry and porosity content of weld deposit.

1. Introduction

The Al–Zn–Mg alloy has gathered wide acceptance in the fabrication of lightweight structures where a high strength to weight ratio is an important criterion for application. During fabrication of various structures of this alloy, such as bridge girders, road and railway transport systems, etc., metal inert gas (MIG) welding is largely used as a means of joining the structural members. However, it has been observed [1–5] that the weldment of Al–Zn–Mg alloy is prone to stress corrosion cracking (SCC) and fatigue failure, especially when the welding is carried out with a large heat input. Earlier investigations show that the presence of a coarse dendritic structure [5] and porosity [3] in the weld deposit affect adversely the fatigue and SCC properties of the weldment of this alloy. The use of a pulse current during welding of this alloy by the MIG process has been found beneficial to improve the mechanical properties of the weld deposit [4, 6, 7] as well as that of the heat-affected zone (HAZ) [8]. This is primarily caused by a good deposition rate at low heat input [9, 10] resulting from interruption in metal deposition [6]. The variation in heat input at different pulse parameters has been found to influence the geometry of the weld deposit [11, 12]. During pulse-current MIG welding the interruption in arcing may cause a fluctuation of pressure within the inert jacket which may result in air aspiration in it and porosity formation in the weld deposit [11, 13]. It is also observed that these aspects are primarily to a great extent sensitive to some pulse parameters such as the mean current and pulse frequency [11, 12]. The change in geometry of the weld deposit as well as its porosity content may have a significant influence on the fatigue properties of Al–Zn–Mg alloy weldment. However, hardly any studies have been reported so far on this aspect in the case of a pulse MIG weld.

In this investigation an attempt was made to study the effect of mean current and pulse frequency on the geometry and porosity content of the weld deposit in pulse-current MIG-welded Al–Zn–Mg alloy. The fatigue life of the weldments has also been determined and correlated with the geometry and porosity content of the weld deposit observed at different pulse parameters.

2. Experimental procedure

The MIG welding of an extruded section (50 mm × 7.0 mm) of Al–Zn–Mg alloys was carried out using 1.6 mm diameter filler wire and commercial argon (99.98%) as shielding gas at a flow rate of 15 l min^{-1}. The chemical composition of the base metal and the filler wire are given in Table I. The welding was carried out by depositing weld metal in the groove as shown schematically in Fig. 1. Prior to welding, the plates were thoroughly cleaned to remove any dirt or grease adhering to the groove surface. During pulse-current welding the mean current was applied at three different levels, e.g. 150 A to obtain a globular metal transfer, 180 A for the transition from globular to spray mode transfer of metal, and 210 A where spray mode transfer of molten filler metal exists. At each level of mean current the pulse frequency was varied to 25, 33, 50 and 100 Hz. For a comparative study the welds were also produced by a conventional continuous current (0 Hz) MIG-welding process using a welding current of the same order as that of the mean current used for pulse-current welding mentioned above. At each level of current, the welding speed was adjusted that during welding at different parameters full penetration in a single pass was obtained. However, at a given mean current during welding at different pulse frequencies, the welding speed was kept constant.

0022–2461/91 $03.00 + .12

TABLE I Chemical composition of base metal and filler wire (wt%)

Material	Al	Zn	Mg	Mn	Fe	Si	Cu	Cr	Ti
Base	Bal.	4.5	1.25	0.45	0.45	0.3	0.15	–	–
Filler	Bal.		4.9	0.7	–	–		0.15	0.15

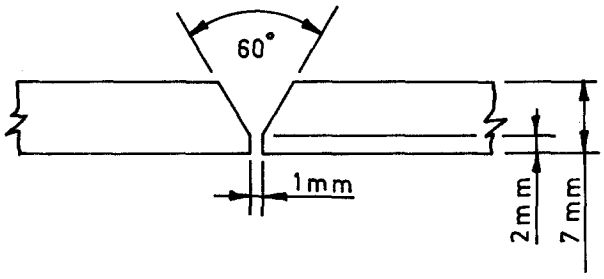

Figure 1 Schematic diagram of the weld groove.

During welding a copper backing plate was used and the whole apparatus was rigidly held in a suitable fixture. During welding the pulse characteristics were recorded with the help of an oscilloscope. The level of current at the desired positions of the pulse and the pulse duration were estimated with the help of a digital oscilloscope. The welding parameters used in this investigation are given in Table II.

Specimens for metallographic examination were collected from the central part of the weldment to ensure a true representation of the weld characteristics. The specimens were machined to remove the bead reinforcement, followed by a further removal of material from both the top and bottom surfaces of the weldment to a depth of about 0.3 mm, so that the error in estimation caused by even a minor irregularity in bead spread could be avoided. The transverse section of the weld was prepared by standard metallographic procedure and suitably etched in Keller's reagent to reveal the microstructure. The weld geometry was estimated by measuring the widths of the top, A, and bottom, B, of the weld under an optical microscope.

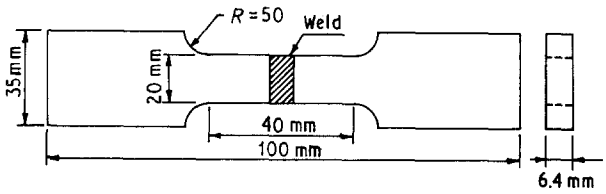

Figure 2 Schematic diagram of the tensile fatigue specimen.

The porosity content of the weld deposit excluding the reinforced region was estimated under an optical microscope by following the standard point-counting method [14]. For this purpose, polished unetched transverse sections of the weld were used.

The specimens for fatigue testing, as schematically shown in Fig. 2, were collected from the weldments after removing its run-on and run-off portions, so that welding under a stable arc condition was ensured. The specimens were fabricated after removing the material to a depth of about 0.3 mm from both the top (excluding reinforced bead) and bottom surfaces of the weldment. Before fabrication of specimens, the weldments were stored at room temperature (295 K) for more than 30 days so that the HAZ (close to the fusion line) could reach a sufficient degree of natural ageing. Fatigue testing was carried out under uniaxial tensile loading, where the mean stress and stress ratio, R, defined as the ratio of minimum to maximum stress, were kept constant at 127.5 $N mm^{-2}$ and 0.5, respectively.

3. Results and discussion

3.1. Geometry of weld deposit

A typical variation in weld geometry on changing the pulse frequency from 0–100 Hz revealed in a transverse section of the joint is shown in Fig. 3 where, the mean current was kept constant at 210 A. It was observed that the variation in pulse frequency had a

TABLE II Welding parameters and specimen designation

Specimen designation	Mean welding current (A)	Base current (A)	Pulse frequency (Hz)	Pulse duration (ms)	Arc voltage (V)	Travel speed (cm min^{-1})
1	150	150	0	6.58	26	27.0
2	150	120	25	6.58	26	27.0
3	150	110	33	6.58	26	27.0
4	150	90	50	6.58	26	27.0
5	150	30	100	6.58	26	27.0
6	180	180	0	6.58	26	35.0
7	180	150	25	6.58	26	35.0
8	180	130	33	6.58	26	35.0
9	180	110	50	6.58	26	35.0
10	180	40	100	6.58	26	35.0
11	210	210	0	6.58	26	40.0
12	210	180	25	6.58	26	40.0
13	210	150	33	6.58	26	40.0
14	210	130	50	6.58	26	40.0
15	210	60	100	6.58	26	40.0

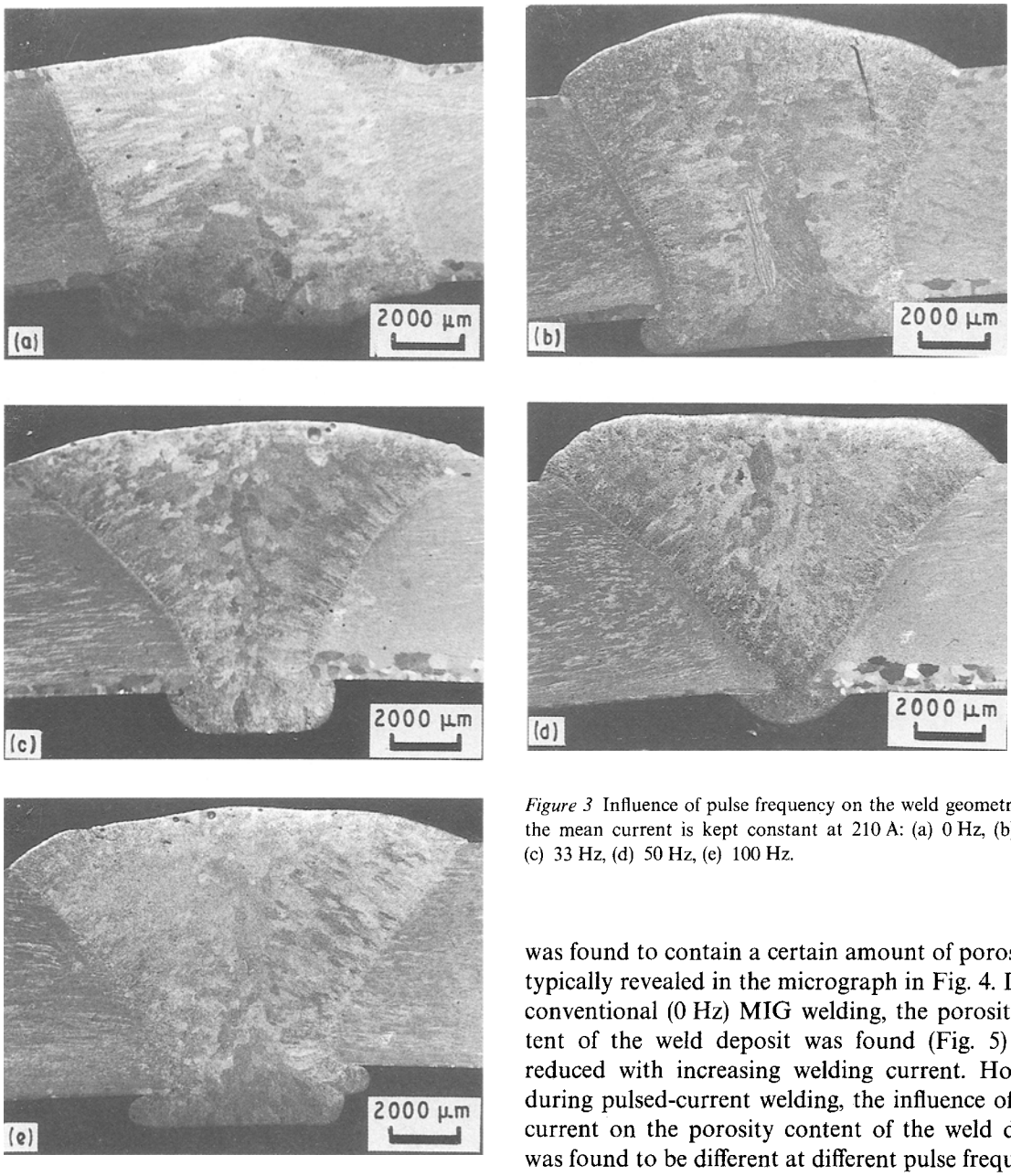

Figure 3 Influence of pulse frequency on the weld geometry where the mean current is kept constant at 210 A: (a) 0 Hz, (b) 25 Hz, (c) 33 Hz, (d) 50 Hz, (e) 100 Hz.

considerable influence on the shape of weld joint. In general, it is marked that the increase in pulse frequency from 0–50 Hz becomes smaller down the root of the weld deposit, followed by a broadening with further increase in pulse frequency to 100 Hz. However, this behaviour has been found to be more pronounced when the mean welding current is higher than the transition level. At different levels of mean current the influence of pulse frequency on the weld geometry estimated by a ratio r, defined as B/A, is presented in Table III.

In agreement with earlier work [12], the variation in weld geometry with changing pulse frequency (Table III) may have been caused by a change in heat input [6, 15] which affected the melting of the base metal.

3.2. Porosity content of the weld deposit

In the present investigation, during welding either by using continuous or pulsed current, the weld deposit was found to contain a certain amount of porosity, as typically revealed in the micrograph in Fig. 4. During conventional (0 Hz) MIG welding, the porosity content of the weld deposit was found (Fig. 5) to be reduced with increasing welding current. However, during pulsed-current welding, the influence of mean current on the porosity content of the weld deposit was found to be different at different pulse frequencies (25, 33, 50 and 100 Hz) as depicted in Figs 6–9, respectively.

In the present work, welding was always carried out under the same conditions of base material, filler wire and shielding gas. Thus the observed variation in

TABLE III Influence of pulse parameters on the weld geometry

Specimen designation	Bead top A (mm)	Bead root, B (mm)	Ratio r (B/A)
2	10.75	5.16	0.48
3	12.02	6.60	0.55
4	11.39	6.45	0.56
5	12.25	7.19	0.58
7	12.04	7.74	0.64
8	12.47	7.095	0.57
9	12.47	6.45	0.52
10	12.47	8.60	0.69
12	10.965	7.525	0.68
13	13.115	3.225	0.24
14	12.47	0.873	0.07
15	13.25	5.3	0.40

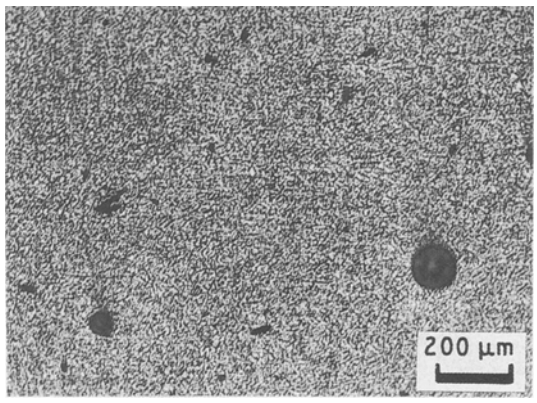

Figure 4 Typical micrograph of weld deposit showing the presence of porosity in it.

porosity content of weld deposit may be assumed to be primarily due to the variation in welding parameters affecting the arc stability, behaviour of metal transfer and the stability of the inert jacket. In the case of conventional MIG welding, an increase in welding current reduces the length of stay of the molten droplet in the arc cavern. Thus it may reduce the absorption of hydrogen and, consequently, the porosity content of the weld deposit. In general, during metal transfer under pulsed current welding, the length of stay of the molten droplet in the arc cavern should be reduced considerably as it is transferred at a current (pulse peak) considerably higher than the mean current. Hence it should reduce gas absorption and the porosity content of the weld deposit. However, during pulsed current welding, in addition to the above phenomenon, the variation in arc pressure leading to the formation of a vortex in inert jacket, resulting in aspiration of air in it, may play an important role in the occurrence of porosity in the weld deposit. During pulsed MIG welding the variation in arc pressure is primarily governed by the ratio of peak current to base current, I_p/I_b. Thus, it can be assumed that the increase in ratio of I_p/I_b will enhance the porosity level of the weld deposit. However, the influence of I_p/I_b on the porosity formation in the weld deposit, studied in the mean current and pulse frequency ranges of 150–210 A and 25–100 Hz, respectively, where both parameters affect I_p/I_b, presented in Fig. 10, interestingly shows that the increase in I_p/I_b to about 6.0 reduces the porosity level of the weld deposit, followed by an enhancement of it with further increase in I_p/I_b. The lowest porosity content of the weld deposit was observed with $I_p/I_b \simeq 6.0$. However, the nature of the curve in Fig. 10 depicts that along with I_p/I_b, there may also be some influence of other parameters, such as pulse off-time, T_o, on the porosity

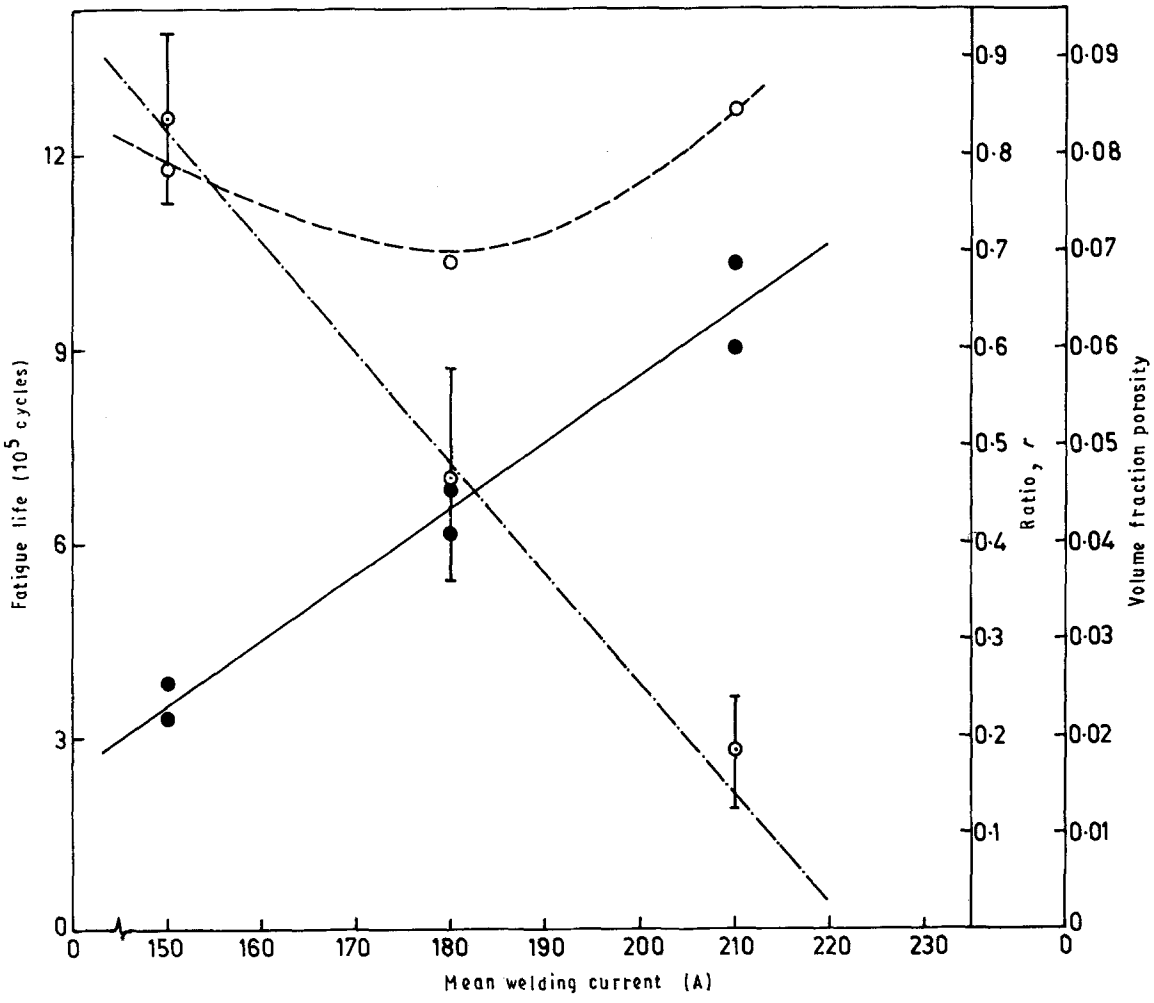

Figure 5 The influence of welding current on (○) weld geometry, r, (⊙) porosity of the weld deposit and (●) fatigue life of the weldment ($R = 0.5$ at mean stress = 127.5 N mm^{-2}) during continuous current welding; pulse frequency = 0 Hz, arc voltage = 26 V.

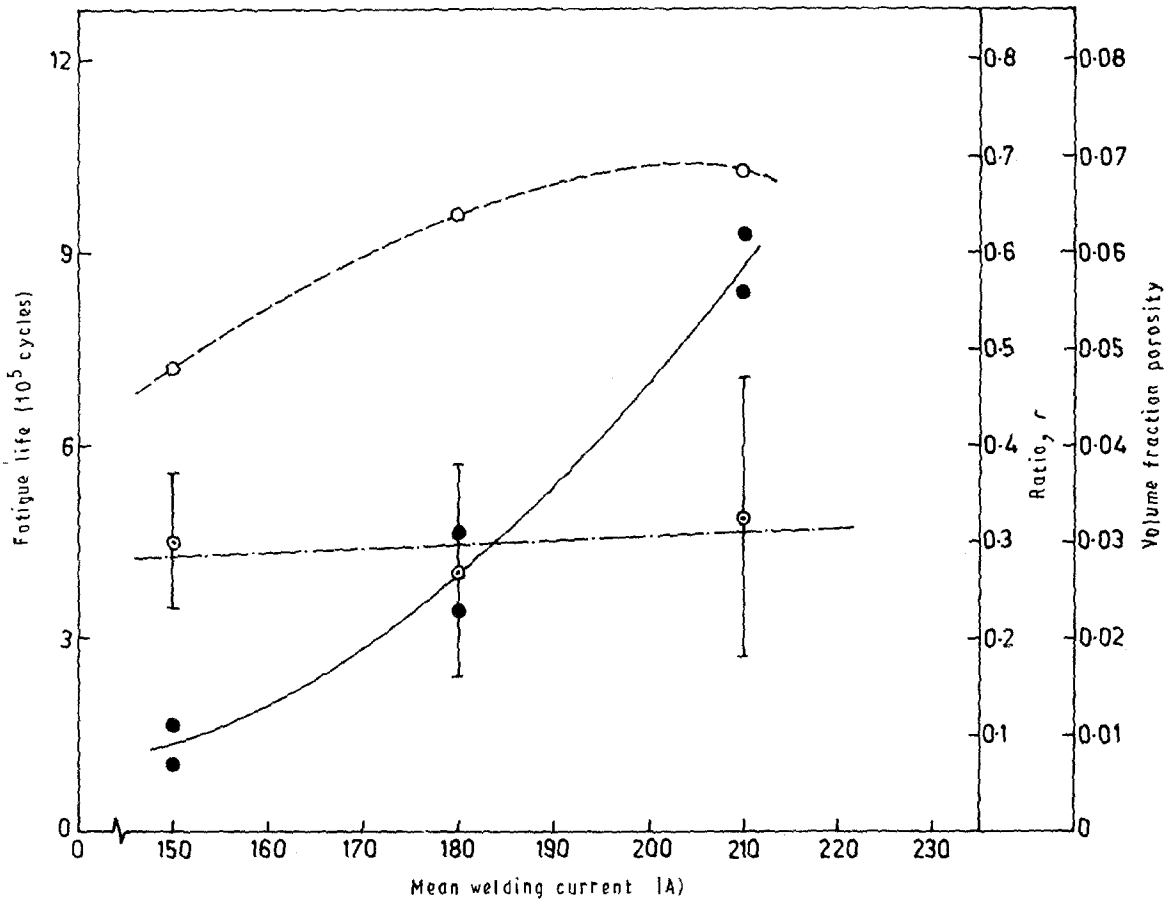

Figure 6 The influence of mean current on (○), weld geometry, *r*, (⊙) porosity of the weld deposit and (●) fatigue life of the weldment ($R = 0.5$, mean stress = 127.5 N mm^{-2}) at a given pulse frequency of 25 Hz, arc voltage = 26 V.

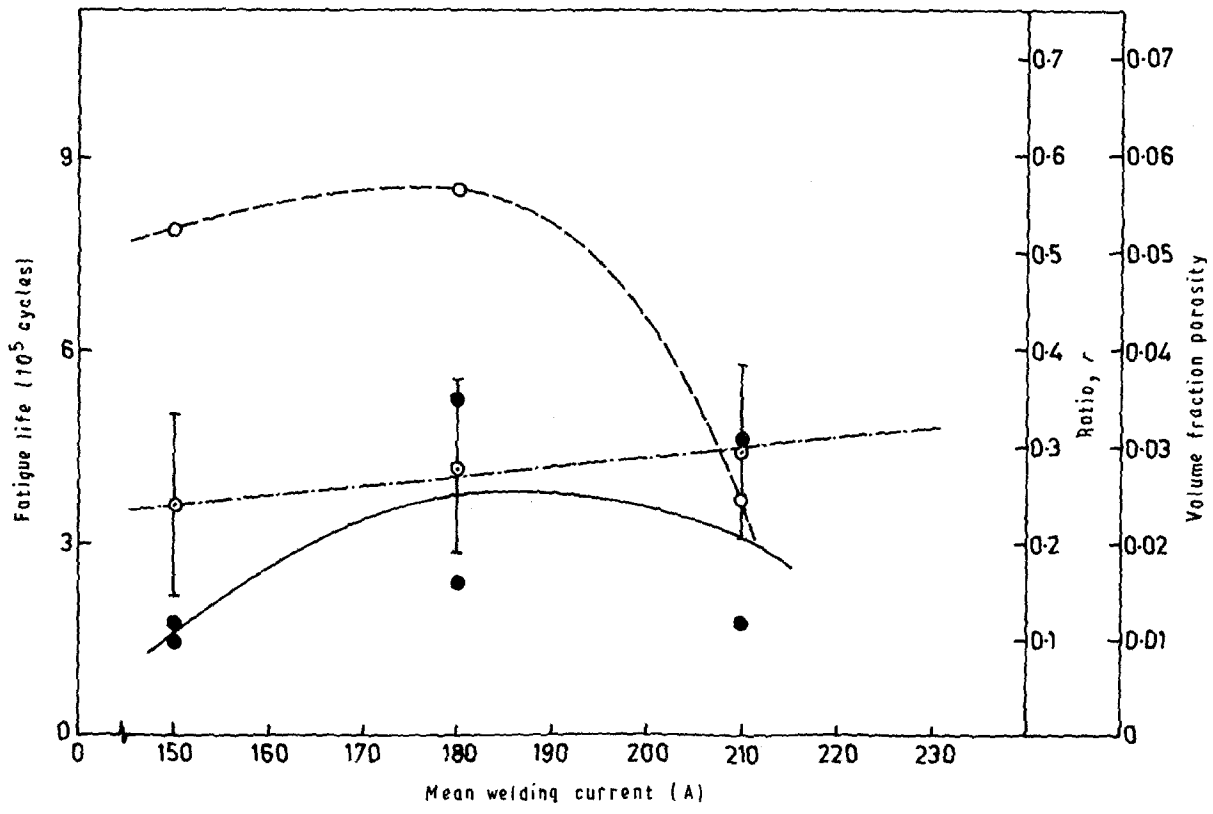

Figure 7 The influence of mean current on (○) weld geometry, *r*, (⊙) porosity of the weld deposit and (●) fatigue life of the weldment ($R = 0.5$, mean stress = 127.5 N mm^{-2}) at a given pulse frequency of 33 Hz, arc voltage = 26 V.

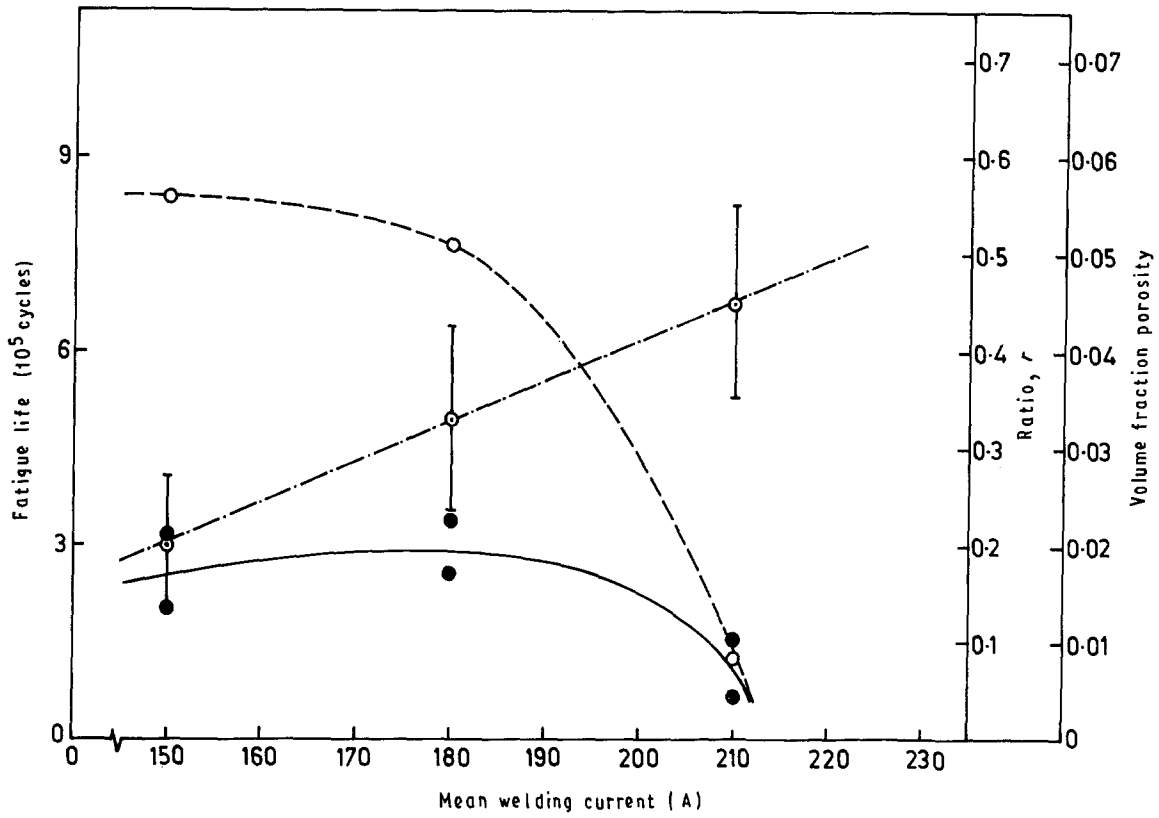

Figure 8 The influence of mean current on (○) weld geometry, r, ⊙ porosity of the weld deposit and (●) fatigue life of the weldment ($R = 0.5$, mean stress = 127.5 N mm^{-1}) at a given pulse frequency of 50 Hz, arc voltage 26 V.

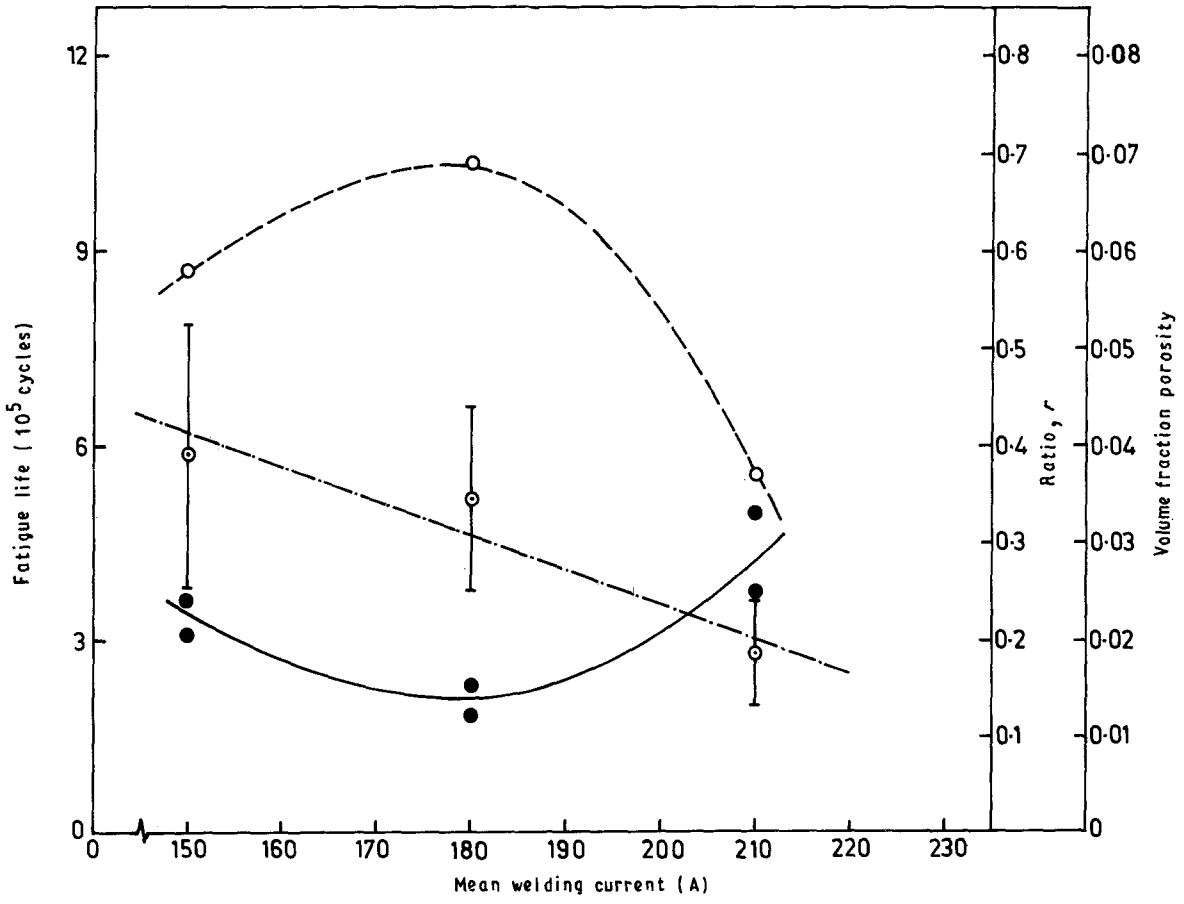

Figure 9 The influence of mean current on (○) weld geometry, r, (⊙) porosity of the weld deposit and (●) fatigue life of the weldment ($R = 0.5$, mean stress = 127.5 N mm^{-2}) at a given pulse frequency of 100 Hz, arc voltage = 26 V.

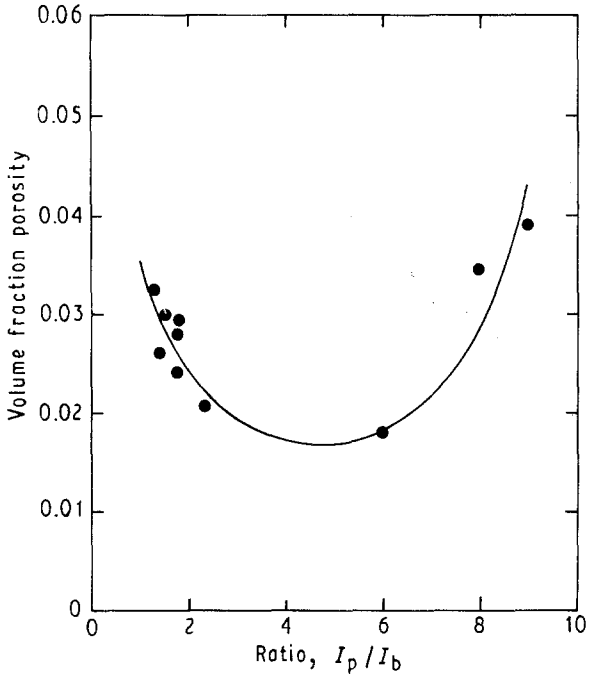

Figure 10 Influence of I_p/I_b on the porosity of the weld deposit, at a mean current of 150–210 A, pulse frequency = 25–100 Hz, pulse duration = 6.58 ms.

content of the weld deposit, which should be investigated further. On increasing the pulse frequency from 25–100 Hz, T_0 decreases from about 29.7–3.4 ms which may affect the prevailing pumping action within the inert jacket caused by fluctuation in arc pressure [7].

3.3. Fatigue properties of the weldment

During fatigue testing of the weldments prepared at different welding parameters, fracture has always been found to occur at the weld centre. The fatigue properties of the weld region are primarily dependent on the geometry of the weld joint governing its residual stresses of a tensile nature and the porosity content of the weld deposit. The influence of welding current during continuous current welding, and the influence of mean current on the fatigue life of the welds during pulsed current welding at different pulse frequencies (25, 33, 50 and 100 Hz) together with their geometry, r, and porosity content, are presented and compared in Figs 5–9. The results presented in Fig. 6 clearly show that the increase in ratio r enhances the fatigue life of the weld, where its porosity content lies within a more

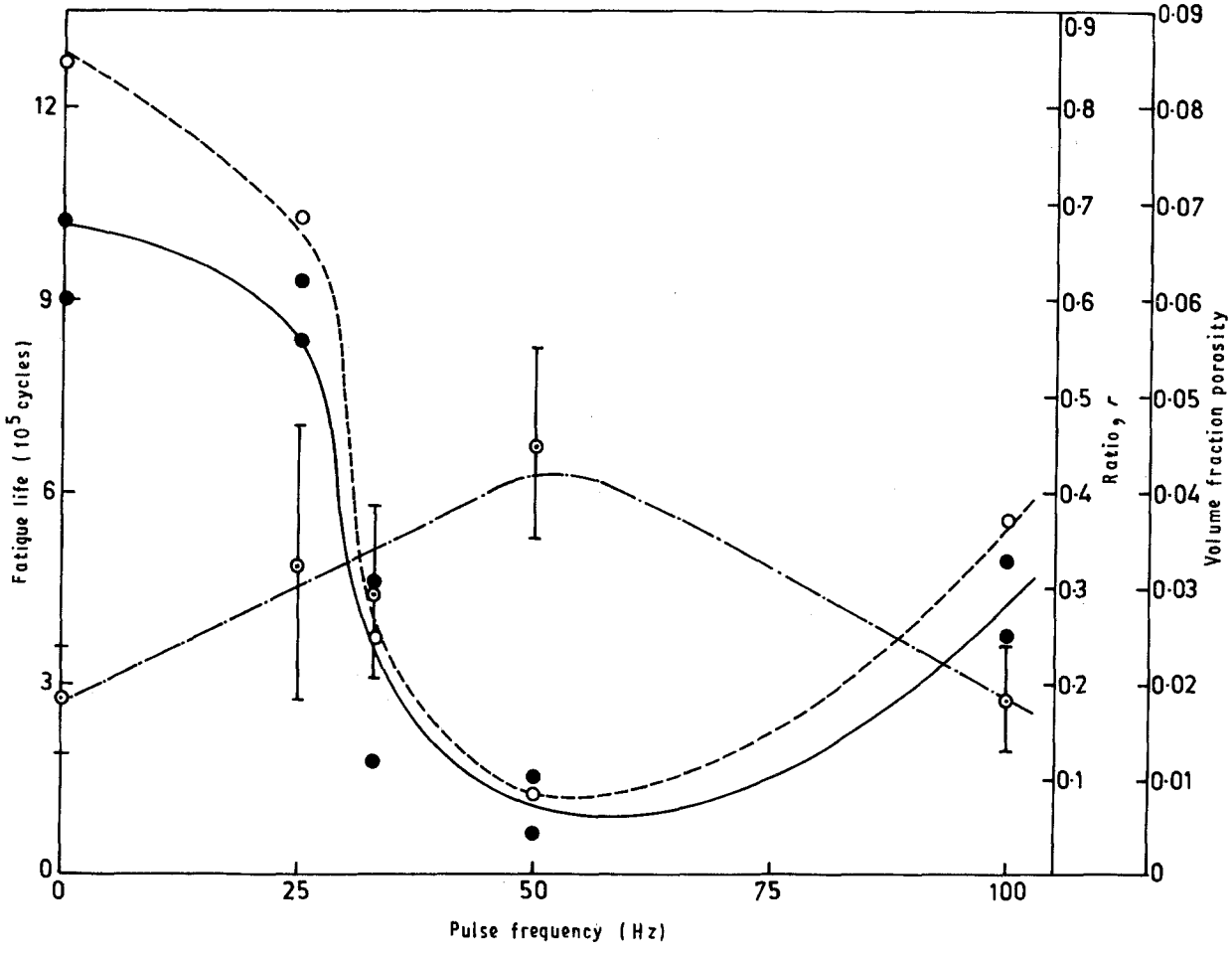

Figure 11 The influence of pulse frequency on (○) weld geometry, r, (⊙) porosity of the weld deposit and (●) fatigue life of the weldment ($R = 0.5$, mean stress = 127.5 N mm^{-2}) at a given mean current of 210 A arc voltage = 26 V, welding speed = 40 cm min^{-1}.

or less similar range. This may have been possible due to reduction in residual stresses of the weld with increasing r resulting from a decrease in cooling rate of the weld deposit caused by comparatively higher heat input and lowering of the area of the base material in contact acting as effective heat sink [12]. At a given mean current of 210 A, the influence of variation in pulse frequency on the ratio r, porosity content and fatigue life of the weld presented in Fig. 11, also supports the dependence of fatigue life on r. In this figure the fatigue curve is found to follow a similar trend to that of the r curve and at a similar level of porosity observed at 0 and 100 Hz the fatigue life is found to be considerably higher at higher r in the case of 0 Hz, than that observed at 100 Hz where r becomes significantly lower. However, while considering the fatigue life of the weld the influence of porosity on it cannot be ignored. In Fig. 9 it is typically observed that in spite of a significant decrease in r with increasing mean current from 180–210 A, the fatigue life of the weld has been relatively increased probably due to the observed reduction in its porosity content. From the discussion on the influence of r and porosity content of the weld on its fatigue life, one can assume that the fatigue life of the weld prepared under different welding conditions presented in Figs 5–9 and 11 has always been suitably determined by the geometry, r, and porosity content of the weld, where the enhancement in r and porosity content increases and decreases the fatigue life, respectively.

In an effort to identify the independent influences of r and porosity content of the weld on its fatigue life, curves are drawn in Figs 12 and 13 showing the effect of r on the fatigue life of the weld when its porosity content remains constant at 3.0 ± 0.8 vol % and the effect of porosity content of the weld on its fatigue life when r lies within 0.56 maximum, respectively. Fig. 12 shows that at a given level of porosity the decrease in r up to about 0.56 reduces the fatigue life of the weld significantly, followed by an insignificant change in it with a further decrease in r. However, at a given range of r lying within 0.56 maximum, the fatigue life of the weld was found (Fig. 13) to decrease significantly with increasing porosity content up to about 3.0 vol %, followed by a moderate decrease with a further increase in porosity level. The correlation between the fatigue life (N cycle) and porosity content (P vol %) of the weld having a coefficient of correlation of about 65%, can be expressed as

$$N = 487\,258.7 - 256\,771.4 \ln P \qquad (1)$$

The scattering of results observed in Figs 12 and 13, causing a comparatively low coefficient of correlation of equation 1 may have resulted from the nature of the distribution of porosity in the matrix. The presence of porosity at or close to the specimen surface acts as a potential site for crack initiation, as shown typically in the micrograph and fractograph of the fatigue specimens presented in Figs 14 and 15, respectively, and thus reduces the fatigue life significantly. However, the

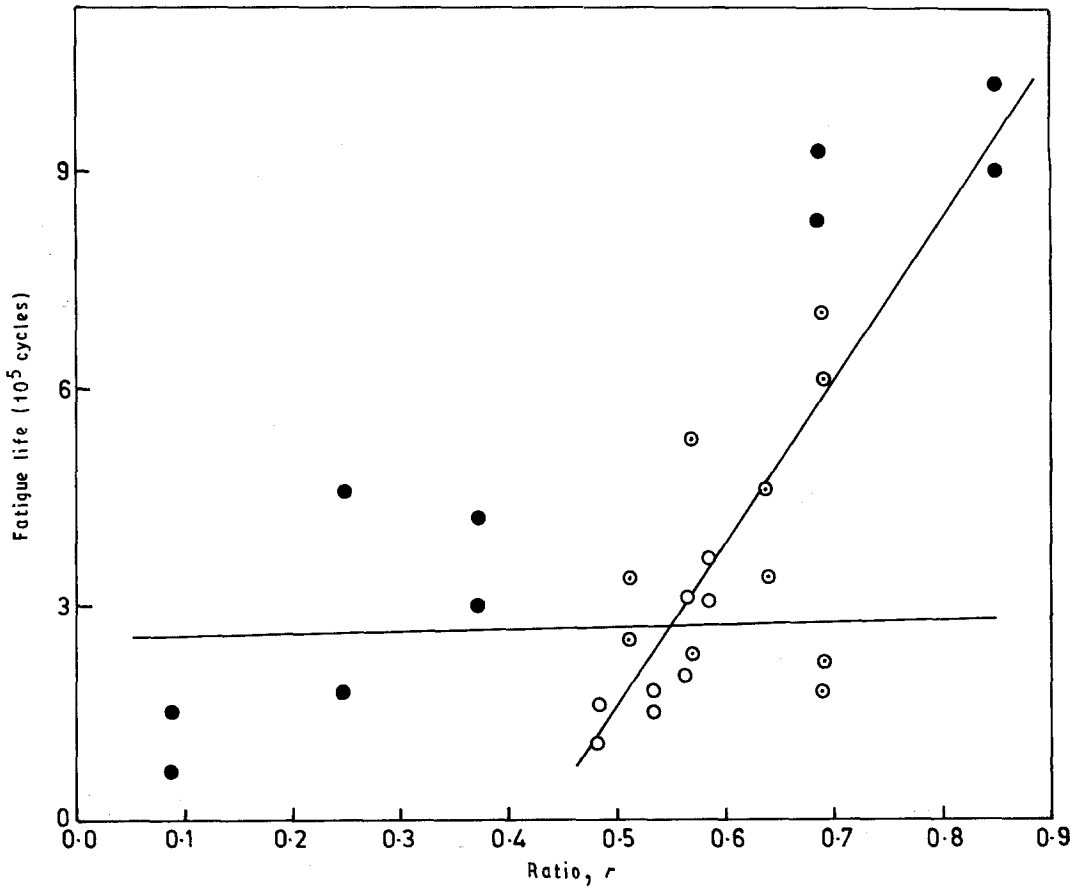

Figure 12 The effect of weld geometry on the fatigue life of the weldment with 3 ± 0.8 vol % porosity. Mean current/welding speeds: (○) 150 A/27 cm min^{-1}, (⊙) 180 A/35 cm min^{-1}, (●) 210 A/40 cm min^{-1}.

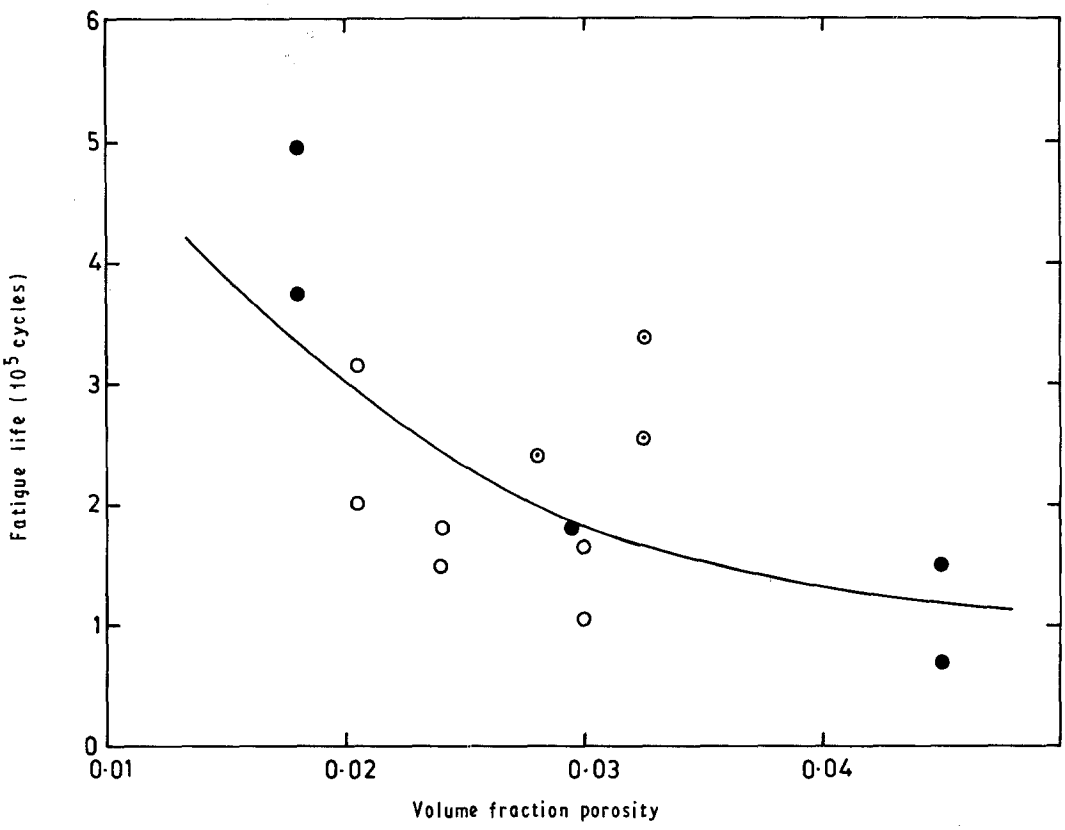

Figure 13 The influence of porosity of the weld deposit on the fatigue life of the weldment. r within 0.56 (max.). Mean current/welding speed: (○) 150 A/27 cm min^{-1}; (⊙) 180 A/35 cm min^{-1}, (●) 210 A/40 cm min^{-1}.

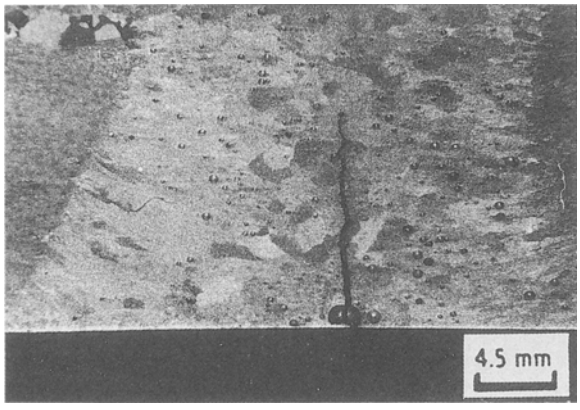

Figure 14 A typical micrograph of a fatigue specimen showing the crack initiation from the pores close to the surface.

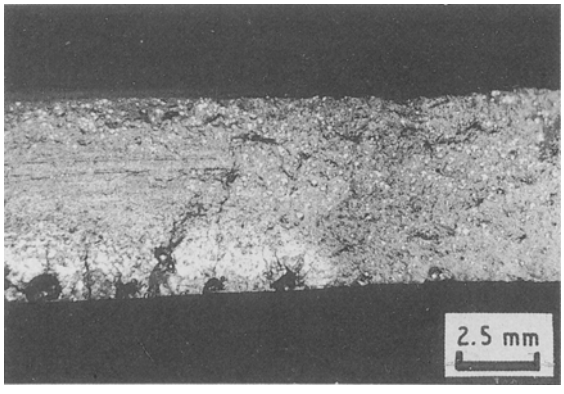

Figure 15 A typical fractograph of a fatigue specimen showing the susceptibility of crack initiation from pores close to the surface.

probability of the presence of porosity at or close to the surface becomes comparatively lower with decreasing porosity of the weld deposit.

4. Conclusions

During pulsed MIG welding of Al–Zn–Mg alloy, the variation in mean current and pulse frequency affects the weld geometry and porosity content of the weld deposit. The geometry and porosity of the weld simultaneously influence the fatigue life of the weldment which generally fails from the weld centre. The increase in the ratio of width of weld root/width of weld top beyond about 0.56 enhances the fatigue life significantly. However, the fatigue life has been found to be reduced significantly with increasing porosity of the weld deposit, up to about 3.0 vol % followed by a comparatively minor change in it, with further increasing porosity.

References

1. R. G. BAKER, *Metal Construct. Brit. Weld. J.* **2** (1970) 65.
2. Discussion Session III, in "Proceedings of the Conference on Weldable Al–Zn–Mg Alloy", 23–25 September 1969, ed. R. G. Baker (The Welding Institute, Cambridge, 1970) p. 126.
3. D. M. ROBKING, N. M. VOROPAI and R. S. KARAMYAN, *Automatic Welding* 21 August (1976) 6.
4. I. B. ROBINSON and F. R. BAYSINGER, *Weld. J. Res. Suppl.* **45** (1966) 433 S.
5. W. GRUH and H. CORDIER, *Z. Metallkde* **55** (1964) 577.
6. P. K. GHOSH, P. C. GUPTA and N. K. JAIN, *Aluminium* **64** (1988) 933.

7. *Idem, Ind. Weld. J.* **21** (1989) 550.
8. P. C. GUPTA, P. K. GHOSH and S. VISSA, in "Proceedings of the International Conference on Welding Technology in Developing Countries: Present Status and Future Needs", University of Roorkee, India, 24–26 September (1988), p. I–71.
9. K. P. BENTLEY, *Welding Metal Fabrication* **34** (1966) 10.
10. J. H. WASZINK and M. J. PIENA, *Welding J. AWS* **65** November (1986) 289-S.
11. R. RATHI, ME dissertation, University of Roorkee, India (1988).
12. P. K. GHOSH, S. R. GUPTA, P. C. GUPTA and R. RATHI, *Trans. JIM* **31** (1990) in press.
13. *Idem, Practical Metallogr.* (1990) in press.
14. R. T. DEHOFF and F. N. RHINES, "Quantitative Microscopy" (McGraw-Hill, New York, 1968) p. 45.
15. K. V. BAGRYANSKII and V. A. ROYANOV, *Svar. Prioz.* **10** (1968) 23.

Received 25 September 1990
and accepted 18 March 1991